International Journal of Robotics and Control Systems
Vol. 2, No. 4, 2022, pp. 709-720
ISSN 2775-2658
http://pubs2.ascee.org/index.php/ijrcs

Numerical Simulation of Non-toxic ZnSe Buffer Layer to Enhance Sb_2S_3 Solar Cell Efficiency Using SCAPS-1D Software

Md. Abdul Halim [1,*], Sunirmal Kumar Biswas [2], Md. Shafiqul Islam [3], Md. Mostak Ahmed [4]

Department of Electrical and Electronic Engineering, Prime University, Mirpur-1, Dhaka-1216, Bangladesh
[1] halimabdul552@gmail.com; [2] sujan.ru.apee@gmail.com; [3] shuvo5684@gmail.com; [4] mostakahmedpu@gmail.com
* Corresponding Author

ARTICLE INFO

Article history
Received July 18, 2022
Revised September 23, 2022
Accepted December 02, 2022

Keywords
Sb_2S_3;
SCAPS-1D;
Optimization;
I-V Measurement;
C-V Curve;
Temperature;
Resistance

ABSTRACT

The use of renewable energy, especially solar photovoltaic, has grown more and more necessary in the context of the diversification of the use of natural resources. Sb_2S_3 is emerged as an attractive candidate for today's thin-film solar cells due to its band gap of 1.65 eV and high absorption coefficient greater than 10^5 cm^{-1}. Cadmium Sulfide is the most commonly used buffer layer material in thin film solar cells, but cadmium is a metal that causes severe toxicity in humans and the environment. This article tried to avoid cadmium for solar cell generation. This paper presents the findings of a computer simulation analysis of a thin film solar cell based on a p-type Sb_2S_3 absorber layer and an n-type ZnSe buffer layer in a structure of (Sb_2S_3/ZnSe/i-ZnO/ZnO: Al) utilizing simulation software (SCAPS-1D). The simulation included detailed configuration optimization for the thickness of the absorber layer, buffer layer, defect density, temperature, and series-shunt resistance. In this work, the Efficiency (η), Fill Factor (FF), Open-circuit Voltage (Voc), and short-circuit current (Jsc) have been measured by varying thickness of absorber layer in the range of 0.5µm to 4 µm and by varying thickness of buffer layer in the range of 0.05 µm to 0.1µm. The optimized solar cell shows an efficiency of 20.03% when the absorber layer thickness is 4µm and the buffer layer thickness is 0.08µm.

1. Introduction

To address the major issues of global warming, there is a desire for sustainable, renewable, cost-effective, and clean energy in today's world. Wind, geothermal, bio, solar energy, and vibration are examples of renewable energy sources [1]. Among all the ambient renewable energy sources, solar energy offers a lot of potential in a variety of applications**.** The materials are crucial things for the generation of a highly efficient solar cell. Some researchers have found some solar energy materials which are based on high light absorption and suitable physical properties to improve the efficiency of the solar cell. A few materials explored for solar cell application are SnS, Cu_2O [2], Cu_2SnS_3 [3], Cu_2GeS_3 [4], GeSe [5], Sb_2S_3 [6], Sb_2Se_3 [7], etc. These materials have shown appropriate physical properties suitable for PV cells. Among these, Sb_2S_3 and Sb_2Se_3 absorber-based solar cells have shown comparatively better PV efficiency, about 6.5%, which has drawn significant attention from a scientific society.

The Sb_2S_3 is a semiconductor material composed of antimony and sulfur. These materials are crucial for terrestrial applications. As a matter of fact, their high efficiency, satisfactory performance for a long time, and low price. These semiconductors exhibit p-type conductivity, a high absorption coefficient, and a direct band gap that makes them appropriate for usage as a thin film absorber layer material [8][9]. Compared to wafer-based crystalline thin film solar cells with polycrystalline Sb_2S_3 absorber layers shows better performance and gives good efficiency. The Sb_2S_3-based solar cells provide better radiation hardness, strong stability, and the highest efficiencies and superb film factor [10]-[13]. The Sb_2S_3 is a compound semiconductor material that lessens the necessity of extensive minority carrier diffusion length of solar cells. Due to the high absorption coefficient, these p-type semiconductor materials are the most promising materials nowadays for thin film photovoltaic technology. An intermediate layer called the buffer layer has been used in this simulation-based work in between the absorber layer and window layer. The window layer has been used here for a specific reason which means it provides structural stability for the device and fixes the electrostatic conditions inside the absorber layer. The prominent compound material CdS could be used as a buffer layer in solar cells. But due to its bad impact on the environment author used Zinc Selenide (ZnSe).

A thin film of Sb_2S_3-based solar cells has been presented in this work using SCAPS-1D to evaluate photovoltaic parameters such as η, FF, $Jsc,$ and Voc at 300K. The impact of the absorber layer and buffer layer on the performance of Sb_2S_3 solar cells has been simulated using SCAPS. Recently a number of research articles have been published on SCAPS-1D software exploring its application in finding efficiencies of different types of solar cells [14]-[16].

As a sustainable source of energy, photovoltaic cell technology has improved greatly in recent years as a result of growing concern over the effects of fossil fuel-based electricity on global warming and climate change. The availability of raw materials may also be a limiting factor for thin film solar cells and also use of CdS as a buffer layer for solar cell generation, but CdS material is not eco-friendly. To overcome these challenging problems, researchers have put their efforts into replacing CdS-based solar cell technology and also using earth-abundant Sb_2S_3 material with one having superior results. The main goal of this study is to see how changing parameters of the absorber layer affect the light conversion efficiency of Sb_2S_3-based thin film solar cells.

The contribution of thin film solar cells to reducing the power shortfall in rural areas without access to the grid is greatly expanding day by day. For the top energy companies, the thin film solar cell revolution has opened up a lot of new commercial options. This study aims to assist the researcher in producing more solar-cell-based energy, which will be used to replace fossil fuels as an environmentally and financially sustainable alternative.

2. Mathematical Modeling and Material Parameters

A compound Antimony tri-sulfide (Sb_2S_3) based solar cell consisting of a p-type absorber layer Sb_2S_3 and n-type buffer layer using ZnSe has been shown in Fig. 1, i-ZnO has been used as a window layer in this solar cell configuration. To simulate and analyze the Sb_2S_3-based solar cell, the author used the SCAPS-1D simulator [17]. SCAPS is a one-dimensional solar cell device simulator invented by a professor at the University of Gent, which is available for the PV research community freely all over the world.

Basic semiconductor equations, the continuity equation, and the Poisson equation can be solved by SCAPS easily for electrons and holes [18].

$$\frac{d^2}{dx^2}\Psi(x) = \frac{e}{\varepsilon_0\varepsilon_r}(p(x) - n(x) + N_D - N_A + \rho_P - \rho_n) \quad (1)$$

From (1), it can easily be said that Ψ is electrostatic potential, e is electrical charge, ε_0 is the vacuum permittivity, ε_r is the relative permittivity, p and n are hole and electron concentrations, N_D is charged impurities of the donor and N_A is acceptor type. There are also holes and electrons distribution ρ_P and ρ_n in this equation.

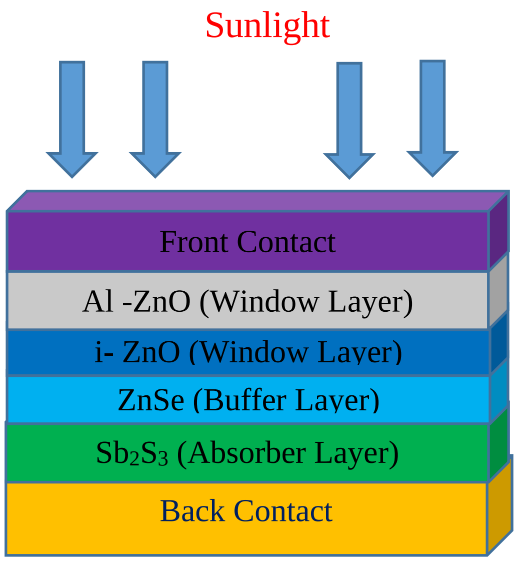

Fig. 1. Schematic diagram of Sb_2S_3-based solar cell

The following (2) and (3) are the continuity equations for electrons and holes:

$$\frac{dJ_n}{dx} = G - R \tag{2}$$

$$\frac{dJ_p}{dx} = G - R \tag{3}$$

Where Jn and Jp represent the electron and hole current densities, R represents the recombination rate, and G is the generation rate. Carrier transportation happens by drift and diffusion in the semiconductor and can be expressed in the following equations:

$$J_n = D_n \frac{d_n}{d_x} + \mu_n n \frac{d\varphi}{d_x} \tag{4}$$

$$J_p = D_p \frac{d_p}{d_x} + \mu_p p \frac{d\varphi}{d_x} \tag{5}$$

The solution of the basic equations of semiconductors has been done using SCAPS in 1 dimension and steady-state conditions. The flow chat has been shown in Fig. 2 for Sb_2S_3 based solar cell. The parameters used in these Sb_2S_3-based solar cells are given below in Table 1.

Table 1. The parameters for the Sb_2S_3-based solar cell at 300K

Parameters	**Sb2S3**	**ZnSe**	**ZnO: Al**	**i-ZnO**
***Eg* (eV)**	**1.62**	**0.08**	**3.5**	**3.3**
εr	7.08	10	9	9
χ (eV)	3.7	2.9	4.2	4.5
μn ($cm^2V^{-1}S^{-1}$)	9.8	50	10^2	10^2
μp ($cm^2V^{-1}S^{-1}$)	10	20	25	25
N_D (cm^{-3})	0	1.5×10^{18}	2.2×10^{18}	1×10^{18}
N_A (cm^{-3})	5.7×10^{15}	0	1.8×10^{19}	1×10^{17}
V_t (cm/s)	1×10^7	1×10^7	1×10^7	1×10^7
V_t (cm/s)	1×10^7	1×10^7	1×10^7	1×10^7

3. Result and Discussion

The main goal of this study is to see how changing parameters of the absorber layer affect the light conversion efficiency of Sb_2S_3-based thin film solar cells. The use of the optimized data will allow us to establish a set of criteria for real-time solar photovoltaic device design with the highest efficiency. This in-depth investigation allowed us to measure the Efficiency (η), Fill Factor (FF), Open-circuit Voltage (Voc), and short-circuit current (Jsc) in the Sb_2S_3 -based thin film solar cell, allowing the research community to develop more efficient solar cell devices [19]. In this paper, Sb_2S_3/ ZnSe/ i-ZnO/ ZnO: Al thin film solar cell has been investigated, and we found an efficiency of 20.03%, as shown in Table 2. The flow chart of Sb2S3 based solar cell is shown in Fig. 2.

Table 2. Photovoltaic parameters for the Sb_2S_3-based solar cell

Device Structure	Open circuit Voltage V_{OC}(V)	Current Density J_{SC} (mA/cm^2)	Fill Factor FF (%)	Efficiency η (%)
ZnO:Al/ i-ZnO/ ZnSe/ Sb_2S_3	1.13	23.89	73.98	20.03

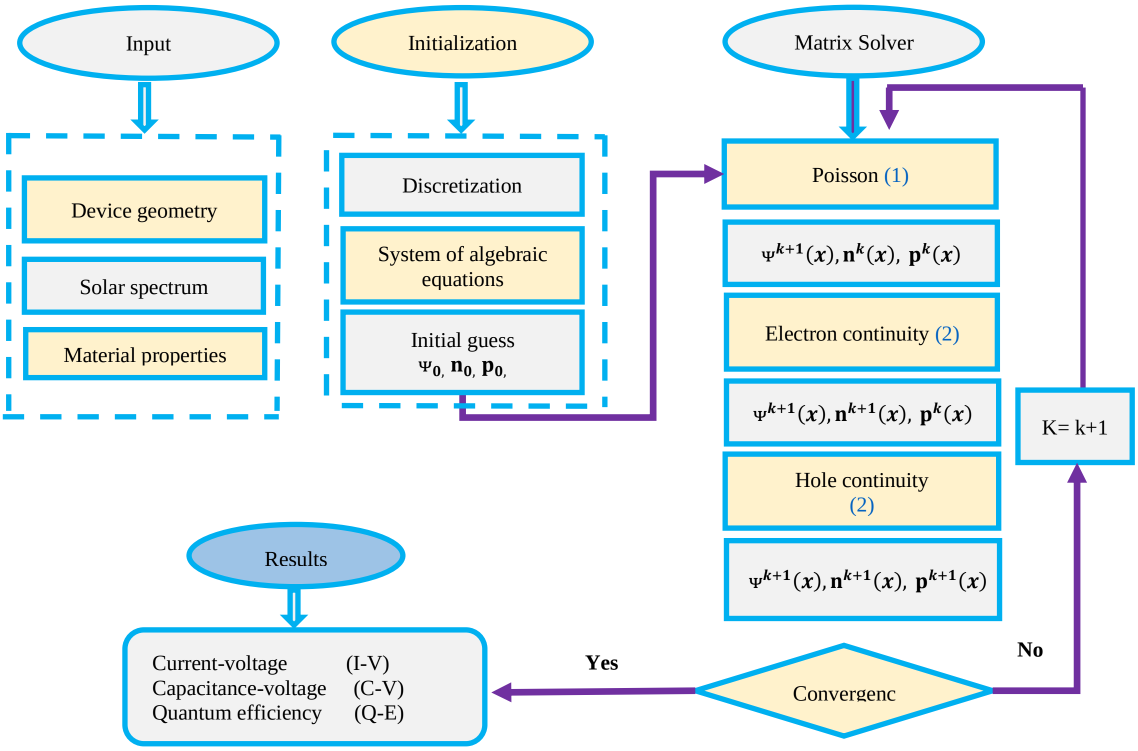

Fig. 2. Flowchart of Sb_2S_3-based solar cell

3.1. Effect of the Absorber Layer and Buffer Layer Thickness on Efficiency in Sb_2S_3-Based Solar Cell

The analysis of the simulated results shows that the best photovoltaic parameters are found by using ZnSe as a buffer layer. To achieve the best performance of the Sb_2S_3-based solar cell, the absorber layer and buffer layer thickness of the cell should be optimized. The impact of absorber layer thickness on solar cell parameters such as open circuit voltage (Voc), short circuit current (Isc), fill factor (FF), and efficiency (%) is thoroughly investigated in this work. Simulated characteristics can be seen in Fig. 3(a, b), Fig. 4(a, b), Fig. 5(a, b), Fig. 6(a, b) for absorber layer from 0.5 µm to 4 .08 µm and buffer layer from 0.02 µm to .14 µm. The increase in efficiency with increasing thickness represents the increase in the generation of the electron-hole pairs in the absorber layer. The efficiency gradually improves as recombination lowers and the extraction rate of electron and hole pairs increases. The rise in optical density is the fundamental cause for the increase in efficiency with increasing thickness [20].

This paper attempted to take values of different parameters by changing the values of the thickness of the absorber layer in the range from 0.5 µm to 4 µm. This paper found an efficiency of 20% when the absorber layer thickness is 4µm shown in Fig. 3(a). The buffer layer thickness is 0.08µm which is shown in Fig. 3(b). Fig. 3(b) indicates that the thickness of the buffer layer is increased, and the efficiency begins to rise. This is because a thinner buffer layer collects the majority of the produced carriers. Short-wavelength photons are absorbed in a greater distance between the window and the absorber junction as the thickness increases [21]. According to the simulation results, if the absorber layer is too thin, it will not be able to absorb all of the incoming light, resulting in low efficiency. Similarly, when the thickness is greater than the optimum value, the photo-produced carrier's travel path is too long, resulting in higher recombination of the generated carrier. When the absorber layer thickness is increased, the carrier recombination rate increases in comparison to the carrier generation rate, resulting in a constant efficiency.

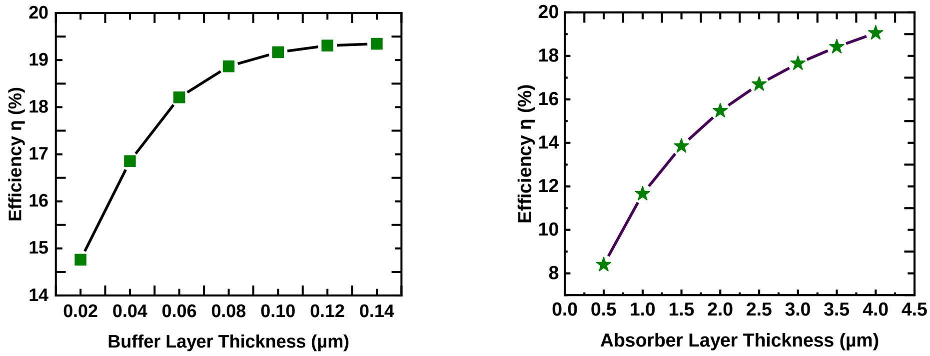

Fig. 3. Effect of the absorber layer and buffer layer thickness on Efficiency

3.2. Effect of the Absorber Layer and Buffer Thickness on Fill Factor in Sb_2S_3-Based Solar Cell

As shown in Fig. 4(a), the fill factor for Sb_2S_3 solar cells improves as the thickness of the absorber layer increases, while it remains constant at thicknesses above 4µm. When the absorber layer thickness is increased, the internal resistance rises. As resistance rises, depletion rises as well, so the fill factor leads to a constant. In Sb2S3-based solar cells, the use of a ZnSe as a buffer layer is required for a reliable and effective hetero-junction. In Fig. 4(b), the effect of buffer layer thickness on the fill factor has been shown. It can be seen that the maximum fill factor has been found when the buffer layer thickness is 0.08µm. After 0.08µm fill factor tends to be constant.

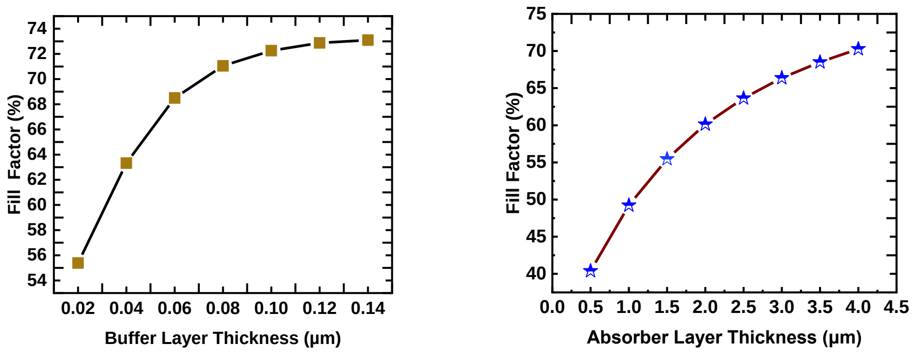

Fig. 4. Effect of the absorber layer and buffer layer thickness on Fill Factor

3.3. The Effects of the Absorber Layer and Buffer Thickness on Current Density in Sb2S3-Based Solar Cell

The carrier recombination rate increases as the absorber layer thickness grow in comparison to the carrier generation rate, as shown in Fig. 5(a). The current increases from 0.5 µm to 4 µm thickness of the absorber layer. However, the current tends to saturate after the 4 µm thickness of the absorber layer. The effect of buffer layer thickness on current density has been shown in Fig. 5(b). The maximum current density of 23.7 mA/cm^2 has been found when the buffer layer thickness is 0.02 µm. But the current density is 23.5 mA/cm^2 when the buffer layer thickness is 0.14µm.

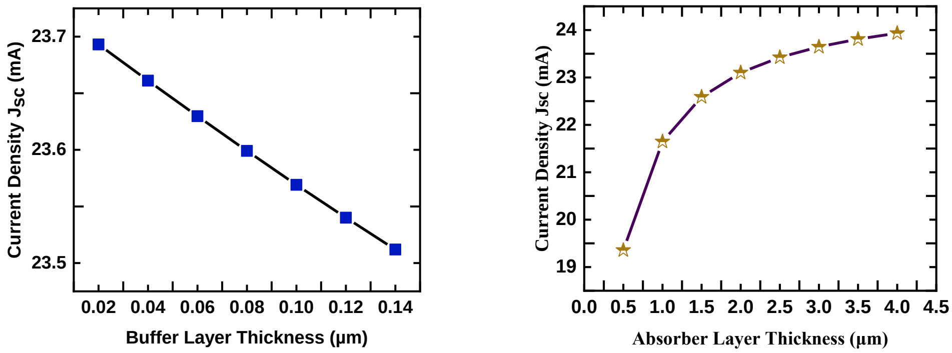

Fig. 5. Effect of the absorber layer and buffer layer thickness on current density

3.4. Effect of the Absorber Layer and Buffer Thickness on Open Circuit Voltage in Sb2S3-Based Solar Cell

As shown in Fig. 6(a), the change in Voc increases as the absorber layer thickness increases due to the effective enhancement of hole mobility. In Fig. 6(b), the effect of buffer layer thickness on open circuit voltage has been shown. Fig. 6(b) shows that open circuit voltage starts increasing with the increase in buffer layer thickness.

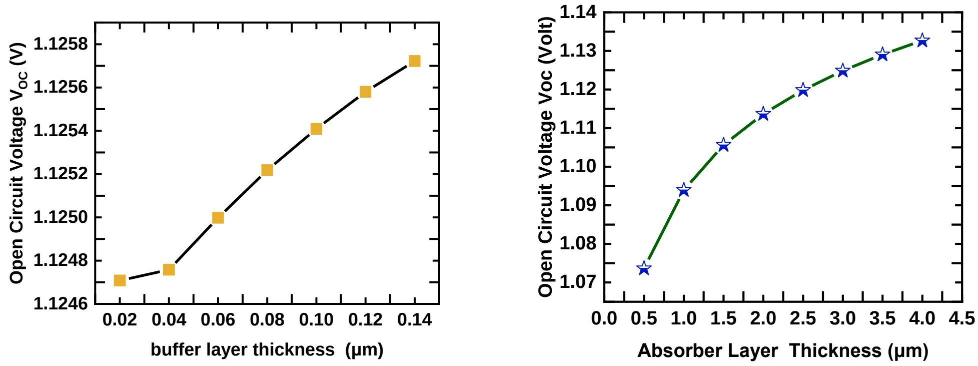

Fig. 6. Effect of the absorber layer and buffer layer thickness on open circuit voltage

3.5. I-V Characteristics Curves of Sb2S3-Based Solar Cell

Fig. 7 depicts the simulated I-V characteristics of a solar cell based on Sb2S3. The four photovoltaic parameters of an Sb2S3-based solar cell Isc, Voc, η and FF has been found from this I-V characteristics curve. According to the diagram, solar cells containing ZnSe as a buffer layer have high conversion efficiency. The maximum efficiency obtained is 20.03% for the Sb2S3 thin film solar cell.

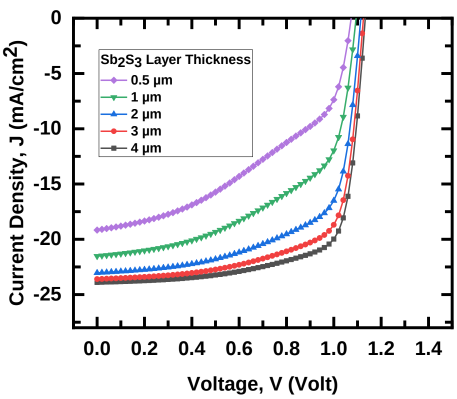

Fig. 7. I-V Characteristics Curve of Sb_2S_3 based solar cell.

3.6. Quantum Efficiency Characteristics Curves for Sb2S3-Based Solar Cell

The ratio of the number of carriers collected by the solar cell to the number of photons with a particular energy incident on the solar cell is known as "quantum efficiency." Quantum efficiency can be expressed in terms of wavelength or energy. The quantum efficiency at a given wavelength is unity if all photons of that wavelength are absorbed and the ensuing minority carriers are collected. It can alternatively be expressed as a function of wavelength or as an amount of energy. The plot of Quantum Efficiency against wavelength in Fig. 8 reveals that more than 90% of the wavelength between 300 nm and 750 nm was radioactively recombined, with less than 10% of the wavelength recombined by other processes.

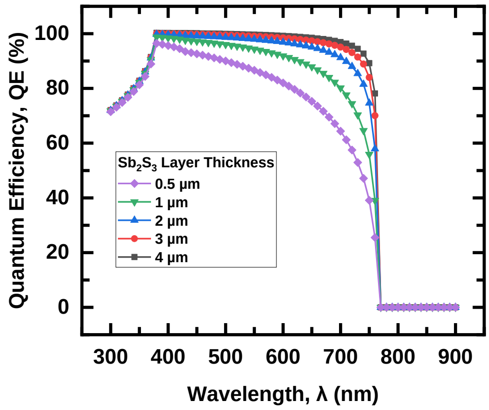

Fig. 8. Quantum Efficiency vs. Wavelength Characteristics Curve of Sb_2S_3 based solar cell.

Quantum efficiency versus wavelength for various absorber thicknesses ranging from 0.5µm to 4 µm is shown in Fig. 8. The quantum efficiency of a solar cell refers to how well it can capture carriers from incident photons of a specific energy. It can be seen that when the absorber thickness decreases, photon absorption at longer wavelengths decreases. This is owing to the fact that the absorber layer contains fewer photo-generated electron-hole pairs. Furthermore, for wavelengths greater than 950 nm, the quantum efficiency is negligible because the light is not absorbed below band gaps at longer low-energy wavelengths [22].

3.7. Voltage and Junction Capacitance Characteristics Curves of Sb2S3-based solar cell

An ideal Schottky diode's capacity increases with the bias voltage and is frequency-independent. The relationship between capacitance (C) and polarization voltage (V) to the Schottky diode is shown in Fig. 9. for several types of solar cell architectures where there is a jumping capacity after V = 0.7 V, with shift curves to higher order capacities containing the superior performance structures.

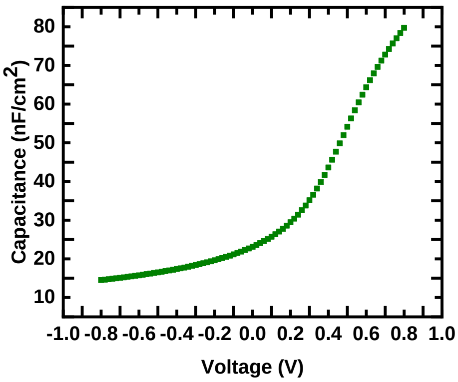

Fig. 9. Voltage vs. Junction Capacitance Characteristics Curve of Sb_2S_3 based solar cell.

3.8. Effect of Temperature on Photovoltaic Parameters of Sb2S3-Based Solar Cell

As shown in Fig. 10, the influence of operating temperature on the photovoltaic performance of the proposed Cd-free Sb2S3 -based Solar Cell is explored when the buffer layer thickness is 0.08 µm with an absorber layer thickness of 4.0 µm. To achieve the stability of the Cd-free Sb2S3 -based Solar Cell, the working temperature has been changed from 250K to 450K. With an increase in operating temperature, Voc dropped dramatically from 1.25V to 0.82V. It is observed in Fig. 10 that Jsc barely increased as the temperature rise. The fill factor increased from 69.5% to 76% with the increase in temperature from 250K to 425K but at 450K fill factor tries to decrease. Efficiencies of 20.52% at temperature 250K have fallen to 15.05% at temperature 450K, which is shown in Fig. 10. The performance of a solar cell device is also influenced by temperature. A solar cell device's testing temperature is usually 300°K. However, the working temperature is higher than 300°K in real-world situations [25]. The temperature of the simulated model was adjusted from 300K to 450K to understand the influence of temperature on the electrical performance of a solar cell. Fig. 9 depicts the changes in the features. The temperature is dropping, with a reduction of 5.42 percent. The increasing temperature may lead to more stress and deformation, resulting in increased interconnectivity between the layers. As the diffusion length decreases, the series resistance rises, lowering the fill factor and efficiency [26]. The simulated model's optimum temperature is adjusted to 300K to ensure high efficiency. The model's maximum possible efficiency is 30.35 percent at this temperature, with a fill factor of 74.94 percent, Jsc= 59.78 mA/cm2, and Voc=0.6774 V.

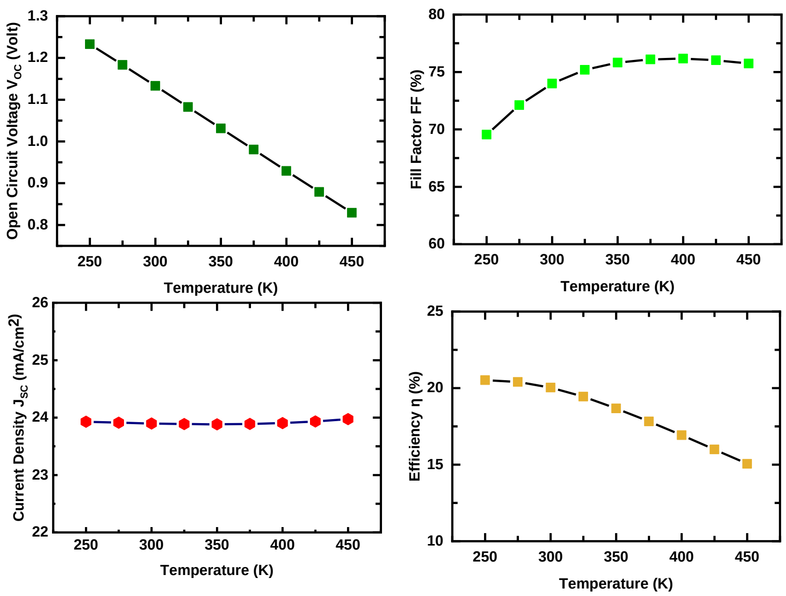

Fig. 10. Effect of temperature on photovoltaic parameter

3.9. Effect of Series Resistance on Photovoltaic Parameters of Sb2S3-Based Solar Cell

Series resistance (Rs) has an effect on solar cell technologies. The bulk resistance, the resistance of the front- and back-surface metallic contacts, and additional circuit resistances from terminals and connectors all contribute to the series resistance. Leakage currents are responsible for the shunt resistance. Non-idealities and contaminants near the pn junction produce partial junction shorting, especially towards the cell borders [23]. It is preferable to get low series and high shunt resistances in order to achieve the goal of high efficiency. Both Jsc and Voc are affected. It's impossible to achieve a perfect FF. Even if we can attain a zero series resistance (Rs) and an infinitely large shunt resistance (Rsh), this is owing to the defective diode behavior of a solar cell [24].

The SCAPS-1D simulator was used to assess the impact of R_S on photovoltaic parameters such Voc, Jsc, FF, and conversion efficiency. The series resistance has been varied from 0Ω to 6Ω, keeping the shunt resistance 10^5Ω as a constant value. With the increase in series resistance, there is almost no change of open circuit voltage and current density, which is shown in Fig. 11. But the Fill Factor has been changed from 73.96% to 65.20% with the enhancement of series resistance. The conversion efficiency of 20.02% has fallen to 17.58% with the increase in series resistance Rs.

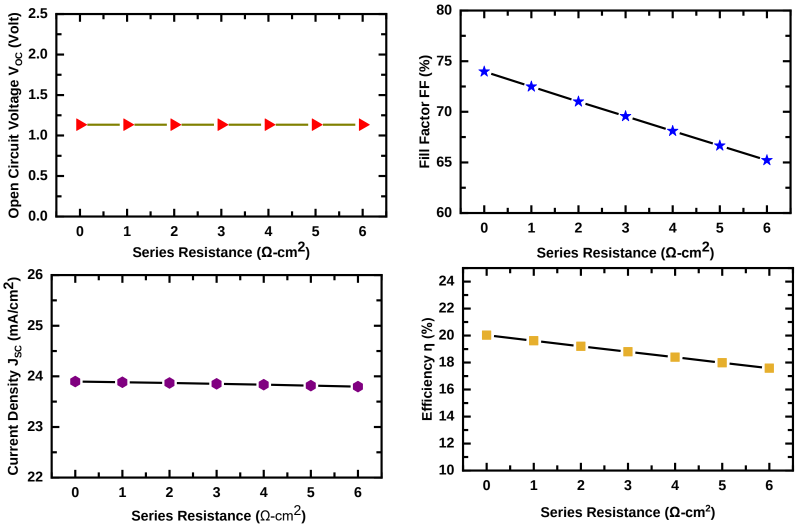

Fig. 11. Effect of Series Resistance on photovoltaic parameter

3.10. Effect of Shunt Resistance on Photovoltaic Parameters of Sb2S3-Based Solar Cell

The effect of shunt resistance R_{Sh} on photovoltaic parameters of Sb2S3-based solar cells has been shown in Fig. 12. The shunt R_{Sh} resistance has been varied from 10Ω to 10^{7}Ω, and series resistance kept 0.5Ω as a constant value. From shunt resistance 10Ω to 10^{2}Ω, there is a little bit of change of open circuit voltage. But from shunt resistance 10^{3}Ω to 10^{7}Ω, there is no change in V_{OH} which is found in Fig. 12. Similarly, from shunt resistance 10Ω to 10^{2}Ω, there is a little bit of change in current density. But from 10^{3}Ω to 10^{7}Ω there is no change in J_{SC}. The Fill Factor has been increased from 25.0271% to 73.2517% with the increase in shunt resistance [27]-[30]. The conversion efficiency has increased from 10Ω to 10^{6}Ω, but after 10^{6}Ω, efficiency tends to be constantly shown in Fig. 12.

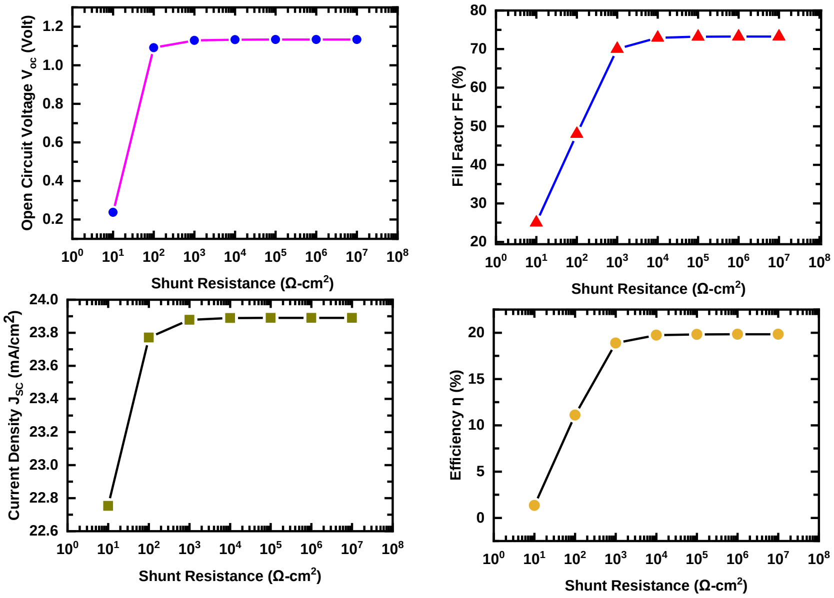

Fig. 12. Effect of Shunt Resistance on photovoltaic parameter

4. Conclusion

The performance of Sb_2S_3-based solar cells has been investigated in this research work using SCAPS-1D. Typical buffer layer CdS can be replaced by compound materials such as Zinc Selenide (ZnSe) and Zinc Sulphide (ZnS). Zinc Selenide (ZnSe) has been used here as an alternative to CdS because of its better performance and availability. The thickness of the absorber in relation to the buffer layer has a significant impact on the efficiency and other photovoltaic parameters of the solar cell, according to the findings. The effect of variation in the thickness of the absorber layer and buffer layer has been investigated in this paper. In this simulation-based work, the Efficiency (η), Fill Factor (FF), Open-circuit Voltage (Voc), and short-circuit current (Jsc) have been investigated and found maximum efficiency of greater than 20% when the absorber layer thickness is 4µm, and buffer layer thickness is 0.08µm. The researchers will be able to build better efficiency Sb2S3 based earth plentiful, non-toxic third-generation solar cells using this paper, which is based on a simulation analysis and optimized parameters.

Acknowledgments

We thankfully acknowledge Dr. Marc Burgelman of the University of Gent in Belgium, who has generously provided the SCAPS simulation program.

References

[1] M. A. Halim, M. M. Hossain, and M. J. Nahar, "Development of a Nonlinear Harvesting Mechanism from Wide Band Vibrations," *International Journal of Robotics and Control Systems*, vol. 2, no. 3, pp. 467-476, 2022, https://doi.org/10.31763/ijrcs.v2i3.524.

[2] Y. S. Lee, et al., "Atomic layer deposited gallium oxide buffer layer enables 1.2 v open-circuit voltage*," in cuprous oxide solar cells Advanced Materials*, vol. 26, pp. 4704–4710, 2019, https://doi.org/10.31763/ijrcs.v2i3.524.

[3] D. M. Berg, et al., "Thin film solar cells based on the ternary compound Cu2SnS3," *Thin Solid Films,* vol. 520, pp. 6291–6294, 2012, https://doi.org/10.1016/j.tsf.2012.05.085.

[4] X. Jin, L. Zhang, G. Jiang, W. Liu, and C. Zhu, 'High open-circuit voltage of ternary Cu2GeS3 thin film solar cells from combustion synthesized Cu-Ge alloy," *Solar Energy Materials and Solar Cells*, vol. 160, pp. 319–327, 2017, https://doi.org/10.1016/j.solmat.2016.11.001.

[5] D-J. Xue, et al., "GeSe thin-film solar cells fabricated by self-regulated rapid thermal sublimation," *Journal of the American Chemical Society*, vol. 139, pp. 958–965, 2017, https://doi.org/10.1021/jacs.6b11705.

[6] S-J. Moon, et al., "Sb2S3 -based mesoscopic solar cell using an organic hole conductor," *The Journal of Physical Chemistry Letters*, vol. 1, no. 10, 1524–1527, 2010, https://doi.org/10.1021/jz100308q.

[7] X. Liu, et al., "Enhanced Sb2Se3 solar cell performance through theory-guided defect control*," Progress in Photovoltaics: Research and Applications*, vol. 25, pp. 861–870, 2017, https://doi.org/10.1002/pip.2900.

[8] P. Jackson, et al., "Effects of heavy alkali elements in Cu(In,Ga)Se_2 solar cells with efficiencies up to 22.6%," *Phys. Status Solidi Rapid Res. Lett.*, vol. 10, no. 8, pp. 583–586, 2016, https://doi.org/10.1002/pssr.201600199.

[9] A. Basak, H. Deka, A. Mondal, and U. P. Singh, "Impact of postdeposition annealing in Cu2SnS3 thin film solar cells prepared by doctor blade method," *Vacuum*, vol. 156, pp. 298–301, https://doi.org/10.1016/j.vacuum.2018.07.049.

[10] I. Repins, et al., "19.9%-efficient ZnO/CdS/CuInGaSe Solar cell with 81.2% fill factor," *Prog Photovolt Res Appl*, pp. 235–239, 2008, https://doi.org/10.1002/pip.822.

[11] J. Lindahl, et al., "Inline Cu(In,Ga)Se2 Co-evaporation for high efficiency solar cells and modules," *IEEE J.Photovolt*, p1100–1105, 2013, https://doi.org/10.1109/JPHOTOV.2013.2256232.

[12] M. Powalla, et al., "High-efficiency Cu (In, Ga) Se2 cells and modules Solar Energy Mater," *Solar Cells*, pp. 51–58, 2013, https://doi.org/10.1016/j.solmat.2013.05.002.

[13] A.Chirila, et al., "Highly efficient Cu(In,Ga)Se2 solar cells grown on flexible polymer films," *Nature Mater*, pp. 857–861, 2011, https://doi.org/10.1038/nmat3122.

[14] A. Basak and U. P. Singh, "Numerical modelling and analysis of earth abundant Sb2S3 and Sb2Se3 based solar cells using SCAPS-1D," *Solar Energy Materials and Solar Cells*, vol. 230, p. 111184, 2021, https://doi.org/10.1016/j.solmat.2021.111184.

[15] M., Kumar, A. Raj, A. Kumar, and A. Anshul, "An optimized lead-free formamidinium Sn-based perovskite solar cell design for high power conversion efficiency by SCAPS simulation," *Optical Materials*, vol. 108, p. 110213, 2020, https://doi.org/10.1016/j.optmat.2020.110213.

[16] N. Singh, A. Agarwal, and M. Agarwal, "Numerical simulation of highly efficient lead-free all-perovskite tandem solar cell," *Solar Energy*, vol. 208, pp. 399-410, 2020, https://doi.org/10.1016/j.solener.2020.08.003.

[17] A. Basak and U. P. Singh, "Numerical modelling and analysis of earth abundant Sb2S3 and Sb2Se3 based solar cells using SCAPS-1D," *Solar Energy Materials and Solar Cells*, vol. 230, p. 111184, 2021, https://doi.org/10.1016/j.solmat.2021.111184.

[18] H. Movla, "Optimization of the CIGS based thin film solar cells: Numerical simulation and analysis," *Optik*, vol. 125, no. 1, pp. 67–70, 2014, https://doi.org/10.1016/j.ijleo.2013.06.034.

[19] A. Sunny, S. Rahman, M. M. Khatun, and S. R. A. Ahmed, "Numerical study of high performance HTL-free CH3NH3SnI3-based perovskite solar cell by SCAPS-1D," *AIP Advances*, vol. 11, no. 6, p. 065102, 2021, https://doi.org/10.1063/5.0049646.

[20] U. Mandadapu, S. V. Vedanayakam and K. Thyagarajan, "Simulation and Analysis of Lead based Perovskite Solar Cell using SCAPS-1D," *Indian Journal of Science and Technology*, vol. 11, March 2017, https://doi.org/10.17485/ijst/2017/v10i11/110721.

[21] P. Chelvanathan, et al. "Performance analysis of copperindium gallium diselenide (CIGS) solar cells with various buffer layers by SCAPS," *Current Applied Physics*, vol. 10, pp. S387-S391, 2010, https://doi.org/10.17485/ijst/2017/v10i11/110721.

[22] A. Sunny, S. Rahman, M. M. Khatun, and S. R. A. Ahmed, "Numerical study of high performance HTL-free CH3NH3SnI3-based perovskite solar cell by SCAPS-1D," *AIP Advances*, vol. 11, no. 6, p. 065102, 2021, https://doi.org/10.1063/5.0049646.

[23] G. Azzouzi, "Study of silicon solar cells performances using the impurity photovoltaic effect," *Doctoral dissertation Supperlattices and Microstructures*, vol. 82, pp. 248-261, 2015, https://doi.org/10.1016/j.egypro.2013.09.005.

[24] O. K. Simya, A. Mahaboobbatcha, and K. Balachander, "A comparative study on the performance of Kesterite based thin film solar cells using SCAPS simulation program," *Superlattices and Microstructures*, vol. 82, pp. 248-261, 2015, https://doi.org/10.1016/j.spmi.2015.02.020.

[25] G. Xosrovashvili and N. E. Gorji," Numerical analysis of TiO2/Cu2ZnSnS4 nanostructured PV using," *Journal of Modern Optics*, vol. 60, no. 11, http://dx.doi.org/10.1080/10.1080/09500340.2014.912001.

[26] A. Raza, H. Shen, A. A. Haidry, L. Sun, R. Liu, and S. Cui, "Studies of Z-scheme WO3-TiO2/Cu2ZnSnS4 ternary nanocomposite with enhanced CO2 photoreduction under visible light irradiation," *Journal of CO2 Utilization*, vol. 37, 260-271, 2020, https://doi.org/10.1016/j.jcou.2019.12.020.

[27] M. Tamilselvan, A. Byregowda, C.-Y. Su, C.-J. Tseng, and A. J. Bhattacharyya, "Planar heterojunction solar cell employing a single-source precursor solution-processed Sb2S3 thin film as the light absorber," *ACS Omega*, vol. 4, pp. 11380–11387, 2019, https://doi.org/10.1021/acsomega.9b01245.

[28] K. Yang, B. Li, and G. Zeng, "Effects of substrate temperature and SnO2 high resistive layer on Sb2Se3 thin film solar cells prepared by pulsed laser deposition," *Sol. Energy Mater. Sol. Cells*, vol. 208, p. 110381, 2020, https://doi.org/10.1016/j.solmat.2019.110381.

[29] Q. Cang, et al., “Enhancement in the efficiency of Sb2Se3 solar cells by adding low lattice mismatch CuSbSe2 hole transport layer,” *Sol. Energy*, vol. 199, pp. 19–25, 2020, https://doi.org/10.1016/j.solener.2020.02.008.

[30] C. Wu, et al., “Interfacial Engineering by Indium-Doped CdS for High Efficiency Solution Processed $Sb_2(S_{1-x}Se_x)_3$ Solar Cells,” *ACS Appl. Mater. Interfaces*, vol. 11, pp. 3207–3213, 2019, https://doi.org/10.1021/acsami.8b18330.